

# A novel solution to the hyperon-puzzle in neutron stars

Arsenia Choroziou and Theodoros Gaitanos\*

Physics Department, School of Physics, Aristotle University of Thessaloniki, 54124 Thessaloniki, Greece

(Dated: February 14, 2024)

Neutron stars offer a great opportunity to study highly compressed hadronic matter experimentally and theoretically. However, the so-called hyperon-puzzle arises at neutron star densities. The hyperon coexistence with other particles in compressed matter softens the equation of state and many widely-accepted models fail to reproduce precise observations of large neutron star masses. Here, we propose a novel mechanism to retain the stiffness of the high density state with hyperons by considering the explicit momentum dependence of their in-medium potentials. Our approach modifies conventional strangeness threshold conditions and generates new threshold effects on hyperons in high-density matter. We demonstrate these effects within the Non-Linear Derivative model, which incorporates baryon momentum-dependent fields based on empirical and microscopic studies. It turns out that even soft momentum-dependent strangeness fields do prohibit their populations in neutron star matter. The generic momentum dependence of strangeness potentials, as modeled by the non-linear derivative approach, is crucial for resolving the long-standing hyperon-puzzle in neutron stars.

*Introduction* – The discovery of massive neutron stars [1–5] has triggered debates in the nuclear/hadron physics and astrophysics communities about the properties of hadrons at high baryon densities and isospin asymmetries [6, 7], particularly related to the hyperon-puzzle [8–11]. At high energy densities, baryons with strangeness content, known as hyperons, can be produced. They soften the hadronic equation of state (EoS) of compressed neutron star (NS) matter and reduce the maximum NS mass below astrophysical observations. Thus, various phenomenological and microscopic nuclear matter approaches have failed to reproduce the observed large neutron star (NS) masses when including strangeness in their descriptions. Proposed solutions include modified vector repulsion of baryons at high densities and the inclusion of additional strangeness exchange mesons in phenomenological approaches [12–15], while microscopic approaches [9, 16–20] predict an explicit momentum dependence (MD) of hyperon potentials based on scattering data.

Inspired by the microscopic MD of in-medium hyperon potentials and the successful predictions of the Non-Linear Derivative (NLD) model for nuclear matter systems [21–23], we extend the NLD approach to  $\beta$ -equilibrated matter with strangeness degrees of freedom. The explicit MD of the hyperon potentials in the NLD model manifests new effects on their threshold conditions. Hyperons can disappear even when the threshold condition is met at zero momentum. Moreover, a soft MD of strangeness potentials may not allow their population in NS matter. We discuss these new momentum-dependent threshold effects within the NLD model, which is based on hyperon potentials in the spirit of the chiral effective field theory ( $\chi$ -EFT). We conclude that within the NLD approach the hyperon-puzzle issue is resolved when considering explicitly momentum-dependent potentials.

*The NLD model* – The NLD formalism [21] is based on the conventional Relativistic Hadro-Dynamics (RHD) [24, 25] with the usual free Lagrangians for the baryons  $\Psi_b$  ( $b = N, Y$  with  $Y$  denoting the hyperons) and those for the exchange

isoscalar-scalar, isoscalar-vector and isovector-vector meson fields  $m = \sigma, \omega, \rho$ . The NLD interaction Lagrangian exhibits the same structure as that in the RHD model, but with non-linear derivative contributions incorporated between the bilinear baryon fields as

$$\mathcal{L}_{int}^m = \sum_b \frac{g_{mb}}{2} \left[ \bar{\Psi}_b \overleftarrow{\mathcal{D}}_b \Gamma_m \Psi_b \varphi_m + \varphi_m \bar{\Psi}_b \Gamma_m \overrightarrow{\mathcal{D}}_b \Psi_b \right], \quad (1)$$

with obvious couplings  $g_{mb}$  and Lorentz-factors  $\Gamma_m = 1, \gamma^\mu, \vec{\tau}\gamma^\mu$  for the various vertices involving the exchange meson fields  $\varphi_m$ . The baryonic non-linear derivative operators  $\mathcal{D}_b$  act on the baryon fields and extend the conventional coupling scheme between baryons and mesons. In momentum space, they are momentum-dependent functions of a common monopole-like form with appropriate cut-off parameters [21]. They regulate the MD of all baryon potentials in consistency with all available empirical and microscopic knowledge. In infinite matter and within the relativistic mean-field approximation the NLD approach yields quasi-free Dirac equations for baryons, featuring explicitly momentum-dependent scalar and vector selfenergies. For instance, the vector component is given by

$$\Sigma_b^\mu(p) = g_{\omega b} \omega^\mu \mathcal{D}_b(p) + \tau_{3b} g_{\rho b} \rho^\mu \mathcal{D}_b(p), \quad (2)$$

with the isospin factor  $\tau_{3b}$  and the regulator  $\mathcal{D}_b(p)$  for a baryon  $b$ . It depends implicitly on the total baryon density  $\rho_B$  too. Similar expressions occur for the scalar selfenergies. For simplicity, the scalar and time-like component of the baryon self-energy will be denoted as  $S_b$  and  $V_b$ , respectively, omitting their explicit MD in most of the expressions. The NLD equations of motion for the  $\sigma$  meson and for the time-like component of the  $\omega$  field read as

$$m_\sigma^2 \sigma + \frac{\partial U}{\partial \sigma} = \sum_b g_{\sigma b} \frac{\kappa}{(2\pi)^3} \int_{|\vec{p}| \leq p_{F_b}} d^3 p \frac{m_b^*}{E_b^*} \mathcal{D}_b(p) \quad (3)$$

$$m_\omega^2 \omega = \sum_b g_{\omega b} \frac{\kappa}{(2\pi)^3} \int_{|\vec{p}| \leq p_{F_b}} d^3 p \mathcal{D}_b(p), \quad (4)$$

\* tgaitano@auth.gr

with the meson masses  $m_{\sigma,\omega}$ , the usual self-interaction term  $U = U(\sigma)$  [26], the spin degeneracy factor  $\kappa = 2$ , the effective mass  $m_b^*(p) = M - S_b(p)$  and the in-medium energy  $E_b^*(p) = \sqrt{m_b^{*2}(p) + p^2}$ . An expression similar to Eq. (4) occurs for the isovector meson  $\rho$ . Finally, the EoS is obtained from the energy density

$$\varepsilon = T^{00} = \sum_b \frac{\kappa}{(2\pi)^3} \int_{|\vec{p}| \leq p_{F_b}} d^3p E_b(p) - \langle \mathcal{L} \rangle \quad (5)$$

with the baryon energy determined from the quasi-free dispersion relation

$$E_b(p) = \sqrt{m_b^{*2}(p) + p^2} + V_b(p) \quad (6)$$

self-consistently due to the explicit momentum dependencies.

Note that the regulators  $\mathcal{D}_b$  enter not only in the baryon self-energies explicitly, Eq. (2), but they show up in the meson-field equations implicitly too, Eqs. (3,4). Thus, within the NLD model, the scalar and, in particular, the vector fields are suppressed (or regulated) with increasing density in a non-linear manner. This in-medium vector suppression was necessary for an adequate description of the EoS and, at the same time, of the in-medium optical potentials [21].

We focus now on the NLD effects to the NS matter including hyperons, that is, hadronic matter in  $\beta$ -equilibrium. Although there are relatively precise empirical analyses available for the MD of the in-medium proton optical potential, the situation in the strangeness sector is still lacking. In particular, available data in the single-strangeness sector allow a theoretical consensus concerning the MD of the single-strangeness ( $\Lambda, \Sigma^{0,\pm}$ )-potentials [27] at matter densities close to saturation. However, in the double-strangeness sector the theoretical uncertainties for the the  $\Xi^{-,0}$ -potentials at finite momentum are still too large [27, 28]. They can lead to a quite ambiguous MD at high densities. A more systematic study concerning the double-strangeness sector is necessary and goes beyond the scope of the present work. Therefore, in order to keep the presentation of the new strangeness threshold effects as transparent as possible, we consider the ( $\Lambda, \Sigma^{0,\pm}$ ) hyperons in this work. We use recent microscopic  $\chi$ -EFT potentials as a reference [18]. The initial NLD results for hyperons were presented in [29]. We have improved and expanded upon them to encompass conditions that are significant for NS matter. The NLD hyperon parameters as shown in Table I are the following: the Lorentz-scalar, isoscalar factor  $\chi_\sigma$  defined by  $g_{\sigma Y} = \chi_\sigma g_{\sigma N}$  ( $\chi_{\omega,\rho}$  are fixed by SU(6)). The cutoffs for the various hyperons, which enter into the regulators  $D_Y(p) = \frac{\Lambda^2}{\Lambda^2 + p^2}$  for the various  $\sigma$ -,  $\omega$ - and  $\rho$ -hyperon interactions [29].

*Momentum-dependent strangeness thresholds* – The key observable for understanding better the strangeness threshold conditions in  $\beta$ -equilibrium and for comparing different models is the Schrödinger-equivalent optical (or simply optical) potential given by

$$U_{opt}^b = -S_b + \frac{E_b}{m_b} V_b + \frac{1}{2m_b} (S_b^2 - V_b^2). \quad (7)$$

Its real part describes the hadronic mean field felt by the baryon  $b$  with a momentum  $p = |\vec{p}|$  relative to the hadronic matter at rest at a given baryon density  $\rho_B$ . For the theoretical description of NS matter we consider the NS composition of the baryons  $b = N, \Lambda, \Sigma^{0,\pm}$  and of the electrons as the only leptonic contribution. The electrons are treated as an ideal Fermi-Gas. Imposing charge neutrality, vanishing strangeness chemical potential due to the infinite time scale of a NS relative to the weak interaction time scale and  $\beta$ -equilibrium, the baryon chemical potentials,  $\mu_b$ , and those of the electrons,  $\mu_e$ , are related through the chemical equilibrium conditions [30] ( $q_b$  is the charge of a baryon  $b$ )

$$\mu_b = \mu_n - q_b \mu_e, \quad \mu_b = \sqrt{p_{F_b}^2 + m_b^{*2}} + V_b, \quad (8)$$

Together with the total baryon density conservation and charge neutrality constraints,

$$\rho_B = \sum_b \rho_b, \quad \sum_b q_b \rho_b - \rho_e = 0, \quad (9)$$

one has to solve self-consistently a set of the non-linear equations (3, 8, 9) for the  $\sigma$ -meson and the two independent chemical potentials  $\mu_n, \mu_e$ . At each iteration step the Fermi-momenta of each particle are calculated from the chemical equilibrium conditions in Eq. (8) as the positive real solutions, that is, the equation  $\mu_b = E_b(p)$  with the solution being the Fermi-momentum  $p_{F_b}$  for a baryon  $b$ . Eqs. (8) indicate the threshold conditions for the particles heavier than the neutron, that is, the strangeness thresholds. Therefore we focus the following discussion on the hyperons (Y). In the NLD model, however, the explicit MD of the effective mass  $m_b^*$  and of the vector selfenergy  $V_b$  will induce modifications of the conventional threshold conditions with new upcoming effects for hyperons.

At first, without any explicit MD in the potential, when the chemical potential  $\mu_n - q_Y \mu_e$  exceeds hyperon's lowest energy, that is

$$\mu_Y = \mu_n - q_Y \mu_e > E_Y(0), \quad (10)$$

a hyperon  $Y$  will be produced with a finite Fermi-momentum  $p_{F_Y}$  as the solution of the equation  $\mu_Y = E_Y(p_{F_Y})$ . The inequality (10) is the conventional threshold condition [30].

With an explicit MD, however, the hyperon selfenergies (or the optical potential) entering in the hyperon energy  $E_Y(p)$  depend explicitly on the hyperon momentum. This generic MD of the fields can induce a non-trivial momentum dependence of the hyperon in-medium energy  $E_Y(p)$  which may differ from the usual monotonically increasing  $p$ -behavior. In other words, the soft/stiff nature of the optical potential versus the momentum at a fixed  $\rho_B$  influences the stiffness of the hyperon in-medium energy as function of momentum. Consequently, it affects the Fermi-momentum value as the solution of  $\mu_Y = E_Y(p_{F_Y})$ , if such a solution exists. Thus, a stiff-like momentum-dependent behavior of the hyperon energy will likely shift the threshold to higher densities, as expected. A weakly soft-like MD of the fields will likely increase the

$\Lambda$ hyperon				$\Sigma^-$ hyperon					$\Sigma^0$ hyperon				$\Sigma^+$ hyperon					
$\chi_\sigma$	$\Lambda_\sigma$	$\Lambda_{\omega_1}$	$\Lambda_{\omega_2}$	$\chi_\sigma$	$\Lambda_\sigma$	$\Lambda_{\omega_1}$	$\Lambda_{\omega_2}$	$\Lambda_\rho$	$\chi_\sigma$	$\Lambda_\sigma$	$\Lambda_{\omega_1}$	$\Lambda_{\omega_2}$	$\chi_\sigma$	$\Lambda_\sigma$	$\Lambda_{\omega_1}$	$\Lambda_{\omega_2}$	$\Lambda_\rho$	
0.83	0.76	0.95	0.79	0.63	0.85	0.95	0.79	0.6	0.6	0.8	0.95	0.79	0.65	0.62	0.95	0.8	0.6	
0.91	0.76	0.95	0.75															

TABLE I. Hyperon parameters: the  $\sigma$ -hyperon scaling factors  $\chi_\sigma$  and the cutoff parameters (in units of GeV)  $\Lambda_\sigma$  ( $\Lambda_1 = \Lambda_2 = \Lambda_\sigma$ ),  $\Lambda_{\omega_{1,2}}$  and  $\Lambda_\rho$  ( $\Lambda_1 = \Lambda_2 = \Lambda_\rho$ ) for the various hyperons. The two parameter sets for the  $\Lambda$  hyperon define the band limits in Fig. 1 (left panels).

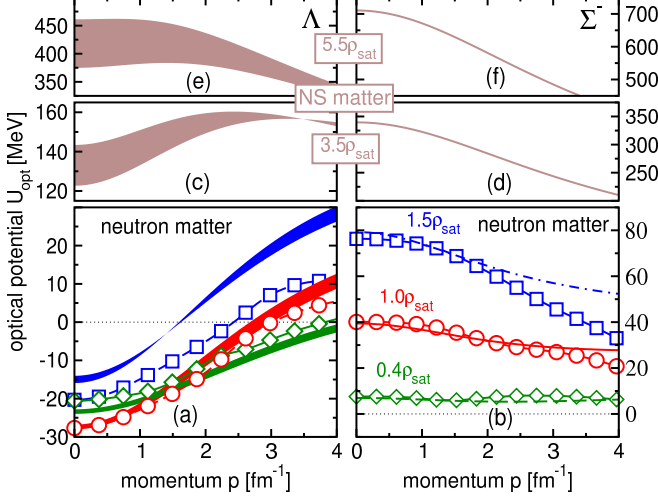


FIG. 1. (Color Online) In-medium optical potentials  $U_{opt}$  for  $\Lambda$  (left) and  $\Sigma^-$  (right) hyperons versus their momentum  $p$ . (a,b) Comparison between NLD (green, red and blue bands) and  $\chi$ -EFT optical potentials [18] (diamond-, circle- and square-symbols) for pure neutron matter at densities of  $\rho_B = 0.062, 0.155$  and  $0.2325$  (in units of  $fm^{-3}$ ), respectively. NLD predictions for NS matter ( $\beta$ -equilibrium) at high densities of  $\rho_B = 0.5 fm^{-3}$  (c,d) and  $\rho_B = 0.8 fm^{-3}$  (e,f) are shown too.

strangeness population, again as expected. However, a particular attention shall be given to the case of a very soft momentum dependent fields. They do reveal new effects on the strangeness thresholds. Very soft momentum-dependent fields may cause a finite hyperon population even if the threshold condition, Eq. (10), is not fulfilled. This is an extreme case and does not occur in the calculations. On the other hand, a very soft MD of the selfenergies can eventually prohibit the hyperon population even with a fulfilled threshold condition at vanishing momentum. This latter case occurs in the calculations and will be particularly discussed in the presentation of the NLD results below.

Therefore, the interplay between momentum dependencies and strangeness population in  $\beta$ -equilibrated compressed matter turns out to be more complex than one would expect. Not only a stiff MD can reduce or forbid the hyperon population, but a soft momentum behavior of the hyperon potential can, in general, prohibit the strangeness production in NS matter too.

*NLD results for neutron star matter* – An appropriate discussion about momentum-dependent threshold effects at high

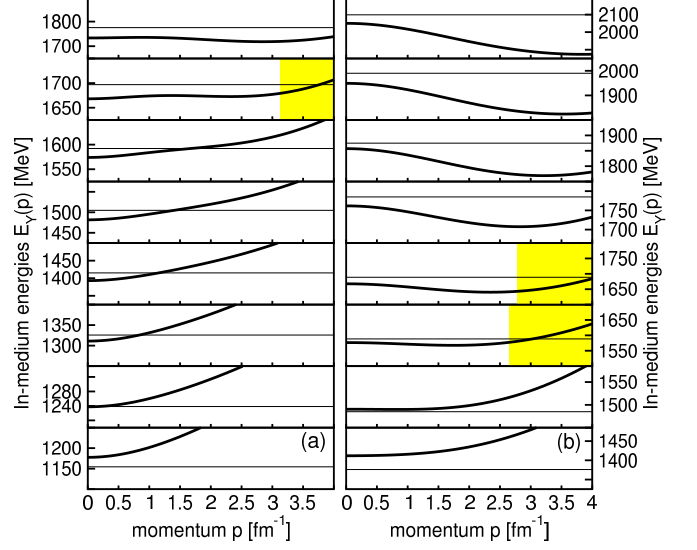


FIG. 2. (Color Online) Demonstration of novel threshold effects for hyperons in the NLD model: the thick curves show the in-medium energies  $E_b(p)$  for  $\Lambda$  (a) and  $\Sigma^-$  (b) hyperons versus their momentum  $p$  for NS matter at baryon densities from  $\rho_B = 0.4 fm^{-3}$  (bottom) up to  $\rho_B = 1.1 fm^{-3}$  (top) in steps of  $0.1 fm^{-3}$ . The thin lines correspond to the thresholds  $\mu_n - q_Y \mu_e$ . The shaded areas indicate the forbidden regions of momenta higher than the Fermi-value at a given baryon density. Even when the population threshold is exceeded, the hyperons don't show up in some cases.

densities requires an adequate MD of the hyperon potentials at saturation density, which is better accessible in theory and eventually in future experiments. This has been realized within the NLD model in Ref. [29]. Here we have refined the MD of the hyperon potentials according to the corresponding  $\chi$ -EFT ones, see Table I. The comparisons between the NLD and the microscopic potentials are summarized in Fig. 1 (panels (a,b)). The NLD cutoffs were adjusted such to reproduce as close as possible the momentum dependence of the  $\chi$ -EFT potentials at the saturation density  $\rho_B = 0.155 fm^{-3}$  only. Although all the  $\Lambda, \Sigma^{0,\pm}$ -hyperons are included in the calculations, we restrict the discussion to the  $\Lambda$  and  $\Sigma^-$  baryons as the most prominent candidates for softening the NS EoS at high baryon densities.

At first, the NLD model gives a quite non-trivial behavior in density and momentum for the  $\Lambda$ - and the  $\Sigma^-$ -potentials in pure neutron matter, which is fully consistent with the  $\chi$ -EFT calculations at the low density region. More specifically, the NLD approach predicts an overall repulsive character of the  $\Sigma^-$ -potential with a soft MD. This is in perfect line with

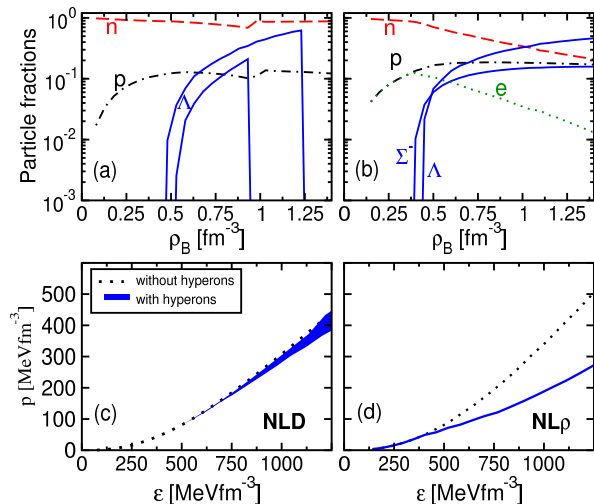


FIG. 3. (Color Online) (a,b) Particle fractions, as indicated, versus the baryon density  $\rho_B$ . (c,d) the NS EoS in terms of the pressure ( $p$ ) versus the energy ( $\epsilon$ ) densities. The results refer to the conventional NL $\rho$  model [32] (b,d) and to the NLD approach (a,c) for NS matter without hyperons (dotted curves in (c,d)) and with the hyperons included (solid curve for NL $\rho$  and filled band for NLD). In the NLD model the electron-curve in (a) equals the  $p$ -curve and the  $\Sigma^-$ -hyperons are not produced. The lower and upper  $\Lambda$ -curves in (a) refer to the lower and upper NS EoS limits in (c).

the microscopic calculations. This soft-like potential behavior versus the  $\Sigma^-$ -momentum is retained and becomes stronger at higher densities (panels (d,f) in Fig. 1).

The  $\Lambda$ -potential, on the other hand, does manifest a more complex MD with increasing densities up to the relevant NS region. We thus give more attention to the adjustment of the NLD  $\Lambda$ -potential to the microscopic results by using different cutoff choices. This results to the filled bands in Fig. 1 (panel (a)). Having in mind that all fits refer to the  $\chi$ -EFT results at saturation density only, the comparison between NLD and  $\chi$ -EFT  $\Lambda$ -potentials is fairly well at the given densities around saturation. It turns out that the NLD model predicts the microscopic in-medium behaviors of the hyperon potentials very well.

The high density sector of the in-medium  $\Lambda$ -potential deserves a particular discussion, since it is the relevant region for NS matter. At first, note that the potential value at zero momentum for  $\rho_B \approx 5\rho_{sat}$  is consistent with recent microscopic studies [9]. As a novel feature, a density-dependent transition from a stiff (Fig. 1, panel (a)) to a soft (Fig. 1, panels (c,e)) momentum-dependent behavior shows up in the  $\Lambda$ -potential. In particular, with increasing baryon density, the  $\Lambda$ -potential exhibits the expected repulsive character for all momenta, but with a decreasing tendency (a very soft behavior) as function of momentum. This is clearly visible at  $\rho_B = 5.5\rho_{sat}$  (panel (e) in Fig. 1). This density-dependent stiffness transition in momentum originates from the NLD regulators. They show up explicitly in the selfenergies and implicitly in the vector-meson source term. Therefore, they soften significantly the MD of the strangeness potential with rising density.

The non-trivial interplay of the hyperon potentials in den-

sity and, in particular, in momentum is manifested in the in-medium energies in Fig. 2. Note again the explicit MD of the selfenergies entering into the hyperon in-medium energy. The  $\Lambda$  in-medium energies with the stiff MD at the low NS density region of  $\rho_B = 0.4 \text{ fm}^{-3}$  cross the corresponding thresholds at momenta below the Fermi-momentum of the given baryon density. That is, they can be populated. The repulsive character of the  $\Sigma^-$  chemical potential does not allow their population in this low NS density region.

With increasing density, however, the momentum-dependent stiffness transition of the hyperon potentials sets in and changes the strangeness population drastically. Indeed, due to the very soft MD of the optical potential the  $\Sigma^-$  in-medium energy does not exceed the corresponding threshold at momenta below the corresponding Fermi-momentum at these high densities, even if the threshold is fulfilled at vanishing momentum. No solution exists and they cannot be populated. The situation is similar for the  $\Lambda$  hyperons. Here the more attractive nature together with the stiff MD of the  $\Lambda$  in-medium energy allows still the  $\Lambda$  population. However, with rising density the stiffness transition is more pronounced for the  $\Lambda$  potential and prevents the production of the  $\Lambda$  baryons again. Note that in some cases the in-medium energies do surpass the threshold line, however, at momenta higher than the allowed maximum value of the Fermi-momentum (indicated with the yellow areas in Fig. 2). Thus, in these cases the  $\Lambda$ -hyperons cannot be populated. It turns out that, within the NLD model, the  $\Sigma^-$ -hyperons cannot be produced at all in NS matter. Only the  $\Lambda$ -hyperons can be populated, however, in a narrow density region.

We discuss now the particle fractions and the NS EoSs within the NLD approach in comparison with a conventional relativistic mean-field (RMF) model. In general, any conventional RMF model results to an EoS softening for NS with hyperons. A stiffness restoration is possible by introducing additional vector-like selfinteraction terms or additional strange vector mesons with more additional parameters [12–15, 31]. For a meaningful comparison with the NLD approach we utilize the conventional NL $\rho$  model from Ref. [32]. It gives similar conditions, i.e., a similar NS EoS for nucleons and comparable hyperon potentials at low momenta relative to NLD. In this way one can reveal better the novel features of the NLD approach. This is shown in Fig. 3 in terms of the particle fractions and NS EoSs. At first, the NL $\rho$  EoS is similar to the NLD EoS for NS matter without hyperons. On the other hand, it is clearly seen that the  $\Lambda$ - as well as the  $\Sigma^-$ -hyperons contribute significantly to the NS composition within the NL $\rho$  model. The NL $\rho$  hyperonic NS EoS is softened largely even with comparable hyperon potentials relative to NLD at low momenta. The situation within the NLD model is very different (panels (a,c) in Fig. 3). The  $\Sigma^-$ -hyperons, in particular the energetically favored  $\Sigma^-$ -hyperons, are prohibited and cannot be populated. The  $\Lambda$ -hyperons are produced above a higher density threshold relative to the NL $\rho$  case, however, with much lower fraction. Note that they disappear again at higher densities due to the stiffness transition effect. As an important consequence, the NLD EoS does not get softened significantly in NS matter by including the hyperons. The

maximum NS mass  $M$  is  $M \approx 2.05M_{\odot}$  without hyperons. This value of  $M \approx 2.05M_{\odot}$  is maintained with the inclusion of hyperons in the NLD model.

*Summary and Conclusions* – In summary, we proposed a solution to the persistent hyperon-puzzle in neutron stars. It is based on the in-medium strangeness MD, realized through the NLD model. This model successfully describes the non-trivial features of empirical and microscopic baryon in-medium optical potentials, and its application to neutron star matter with hyperons is appropriate. The NLD momentum-dependent hyperon fields generate novel effects on their threshold conditions by preventing their population even when the requisite threshold conditions are met. By relying to the MD of the

microscopic  $\chi$ -EFT calculations, the NLD model predicts NS matters with low  $\Lambda$ -hyperon fractions inside a limited density region only with no other hyperons present, resulting in a stiff strangeness NS EoS. It turns out that within the NLD approach the hyperon-puzzle issue is successfully resolved, particularly when considering momentum-dependent hyperon fields.

## ACKNOWLEDGMENTS

We acknowledge Dr. K. Kosmidis for suggestions concerning the numerical treatments and Prof. J. Haidenbauer for valuable discussions and support with the microscopic calculations.

- 
- [1] P. Demorest, T. Pennucci, S. Ransom, M. Roberts and J. Hessels, *Nature* **467**, 1081 (2010).
  - [2] J. Antoniadis, P. C. C. Freire, N. Wex, T. M. Tauris, R. S. Lynch, M. H. van Kerkwijk, M. Kramer, C. Bassa, V. S. Dhillon and T. Driebe, *et al.* *Science* **340**, 6131 (2013).
  - [3] Z. Arzoumanian, A. Brazier, S. Burke-Spolaor, S. Chamberlin, S. Chatterjee, B. Christy, J. M. Cordes, N. J. Cornish, F. Crawford, H. T. Cromartie, *et al.*, *Astrophys. J. Suppl. Ser.* **235**, 37 (2018).
  - [4] H. T. Cromartie, E. Fonseca, S. M. Ransom, P. B. Demorest, Z. Arzoumanian, H. Blumer, P. R. Brook, M. E. DeCesar, T. Dolch, J. A. Ellis, *et al.* *Nat Astron* **4**, 72 (2020).
  - [5] R. W. Romani, D. Kandel, A. V. Filippenko, Th. G. Brink, WeiKang Zheng, *Astrophys. J. Lett.* **934**, L17 (2022).
  - [6] A. W. Steiner, J. M. Lattimer and E. F. Brown, *Astrophys. J. Lett.* **765**, L5 (2013).
  - [7] J. M. Lattimer, *Ann. Rev. Nucl. Part. Sci.* **71**, 433 (2021).
  - [8] D. Lonardoni, A. Lovato, S. Gandolfi and F. Pederiva, *Phys. Rev. Lett.* **114**, no.9, 092301 (2015).
  - [9] D. Gerstung, N. Kaiser and W. Weise, *Eur. Phys. J. A* **56**, no.6, 175 (2020).
  - [10] I. Vidana, D. Logoteta, C. Providencia, A. Polls and I. Bombaci, *EPL* **94**, no.1, 11002 (2011).
  - [11] S. Weissenborn, D. Chatterjee and J. Schaffner-Bielich, *Phys. Rev. C* **85**, no.6, 065802 (2012) [erratum: *Phys. Rev. C* **90**, no.1, 019904 (2014)].
  - [12] I. Bednarek, P. Haensel, J. L. Zdunik, M. Bejger and R. Manka, *Astron. Astrophys.* **543**, A157 (2012).
  - [13] S. Weissenborn, D. Chatterjee and J. Schaffner-Bielich, *Nucl. Phys. A* **881**, 62 (2012).
  - [14] M. Oertel, C. Providencia, F. Gulminelli, Ad R. Raduta *J.Phys.G:Nucl. Part. Phys.* **42**, 075202 (2015).
  - [15] K. A. Maslov, E. E. Kolomeitsev and D. N. Voskresensky, *Phys. Lett. B* **748**, 369 (2015).
  - [16] D. Logoteta, I. Vidana and I. Bombaci, *Eur. Phys. J. A* **55**, no.11, 207 (2019).
  - [17] D. Chatterjee and I. Vidaña, *Eur. Phys. J. A* **52**, no.2, 29 (2016).
  - [18] S. Petschauer, J. Haidenbauer, N. Kaiser, U. G. Meißner and W. Weise, *Eur. Phys. J. A* **52**, no.1, 15 (2016).
  - [19] J. Haidenbauer, U. G. Meißner, A. Nogga and H. Le, *Eur. Phys. J. A* **59**, no.3, 63 (2023).
  - [20] Y. Fujiwara, Y. Suzuki and C. Nakamoto, *Prog. Part. Nucl. Phys.* **58**, 439-520 (2007).
  - [21] T. Gaitanos and M. Kaskulov, *Nucl. Phys. A* **899**, 133 (2013).
  - [22] T. Gaitanos, M. Kaskulov, *Nucl. Phys. A* **878**, 49 (2012).
  - [23] T. Gaitanos, M. Kaskulov, *Nucl. Phys. A* **940**, 181 (2015).
  - [24] B. D. Serot and J. D. Walecka, *Adv. Nucl. Phys.* **16**, 1 (1986).
  - [25] J. Boguta and A. Bodmer, *Nucl. Phys. A* **292**, 413 (1977).
  - [26] J. Boguta and H. Stoecker, *Phys. Lett. B* **120**, 289 (1983).
  - [27] M. Kohno, *Phys. Rev. C* **81**, 014003 (2010).
  - [28] T. Inoue [LATTICE-HALQCD], *PoS INPC2016*, 277 (2016); T. Inoue [HAL QCD], *AIP Conf. Proc.* 2130(1), 020002 (2019).
  - [29] T. Gaitanos and A. Chorozydou, *Nucl. Phys. A* **1008**, 122153 (2021).
  - [30] N. Glendenning *Astrophys. J.* **293**, 470 (1985).
  - [31] C. Providencia and A. Rabhi, *Phys. Rev. C* **87**, 055801 (2013).
  - [32] D. P. Menezes, C. Providencia, *Phys. Rev. C* **70**, 058801 (2004).